Journal of Hazardous Materials 184 (2010) 724–730

Contents lists available at ScienceDirect

Journal of Hazardous Materials

journal homepage: www.elsevier.com/locate/jhazmat

Entrapment of nanoscale zero-valent iron in chitosan beads for hexavalent chromium removal from wastewater

Tingyi Liu, Lin Zhao*, Desheng Sun, Xin Tan

School of Environmental Science and Engineering, Tianjin University, No. 92, Weijin Rd., Nankai District, Tianjin 300072, China

ARTICLE INFO

Article history:
Received 14 July 2010
Received in revised form 23 August 2010
Accepted 25 August 2010
Available online 19 September 2010

Keywords:
Nanoscale zero-valent iron (NZVI)
Chitosan
CS-NZVI beads
Hexavalent chromium

ABSTRACT

Nanoscale zero-valent iron (NZVI) was successfully entrapped in chitosan (CS) beads for reduction of Cr (VI) from wastewater. The removal mechanism may include both physical adsorption of Cr (VI) on the surface or inside of CS-NZVI beads and subsequent reduction of Cr (VI) to Cr (III). The free amino groups and hydroxyl groups on CS may contribute little to hinder the formation of Fe(III)–Cr(III) precipitate. Entrapment of NZVI in CS beads prevents the particles from aggregation and oxidation. The results indicate that there is no significant difference between the reaction rates of bare NZVI and entrapped NZVI. Cr (VI) reduction kinetics follows a pseudo-first-order rate expression. The reduction capacity for Cr (VI) increases with increasing temperature and NZVI dosage but decreases with the increase in initial concentration of Cr (VI) and pH values. This study demonstrates that entrapment of NZVI in CS beads has the potential to become a promising technique for in situ groundwater remediation.

1. Introduction

Chromium is a potential carcinogen and often causes both short term and long term adverse effects to humans, animals, and plants [1]. Chromium is widely detected in surface water and groundwater, and its levels in some wastewater are higher than the action level of 0.1 mg/L [2]. Chromium in natural water exists in two stable states, hexavalent [Cr (VI)] and trivalent [Cr (III)]. Cr (VI) species such as chromate (CrO_4^{2-}, $HCrO_4^-$) and dichromate ($Cr_2O_7^{2-}$) are highly soluble and mobile in aqueous solution and are of great environmental concern.

In recent years, nanoscale zero-valent iron (NZVI) has been used for the removal of various wastewater contaminants including nitrate [3], chlorinated compounds [4], heavy metals [5,6], and so on. However, the agglomeration, oxidation by non-target compounds and higher mobility in the aqueous solution are the major challenges for NZVI use in environmental remediation [7]. To overcome these problems, NZVI has been modified using surface stabilisers such as Tween-20 [8], oil [9], noble metals [10], starch [11], guar gum [12], and chitosan [13]. Sodium carboxymethyl cellulose, polyacrylic acid, and hydrophilic carbon have been used to improve the transport of NZVI in soil [14]. In order to enhance the stability in the air, NZVI was supported on PolyFlo resin [15]. Recently, NZVI particles were effectively entrapped in calcium alginate beads without significant reduction in their reactivity [16]. Entrapment of NZVI in porous beads will be a promising technology in the application of NZVI particles. This study presents work to entrap NZVI in a porous polymer.

Chitosan (CS) is a reproducible resource and environmental friendly material which can be completely degraded by the chitosan enzyme, bacteriolysis enzyme and animalcule [17]. Particularly, chitosan, a derivative from N-deacetylation of chitin, has been found to be capable of chemically or physically adsorbing various heavy metal ions [18]. Previous investigations have demonstrated that chitosan dydrogel beads are porous and stable in aqueous phase, and effective to remove copper, mercury ions, and chromium [19,20]. However, there are scarce studies of reduction of Cr (VI) using entrapment of nanoscale zero-valent iron in CS beads (CS-NZVI beads).

The goal of this study is to prepare a new class of CS-NZVI beads for the remediation of Cr (VI) in wastewater. The main objectives are to: (1) synthesize and characterize CS-NZVI beads, (2) test the role of chitosan in Cr (VI) reduction by CS-NZVI beads, as well as elemental composition of final products, and (3) evaluate the influence of different factors on the Cr (VI) removal by CS-NZVI beads.

2. Materials and methods

2.1. Chemicals and materials

Chitosan flakes (85% deacetylated) and cellulose power (20 μm) were purchased from Sigma Co. NZVI particles with a mean diameter of 65.3 nm were purchased from Nanjing Emperor Nano Material Co. Ltd. Cr (VI) standard solution (20 mg/L), anhydrous

* Corresponding author. Tel.: +86 22 27405495; fax: +86 22 27405495.
E-mail address: zhaolin@tju.edu.cn (L. Zhao).

0304-3894/$ – see front matter.
doi:10.1016/j.jhazmat.2010.08.099

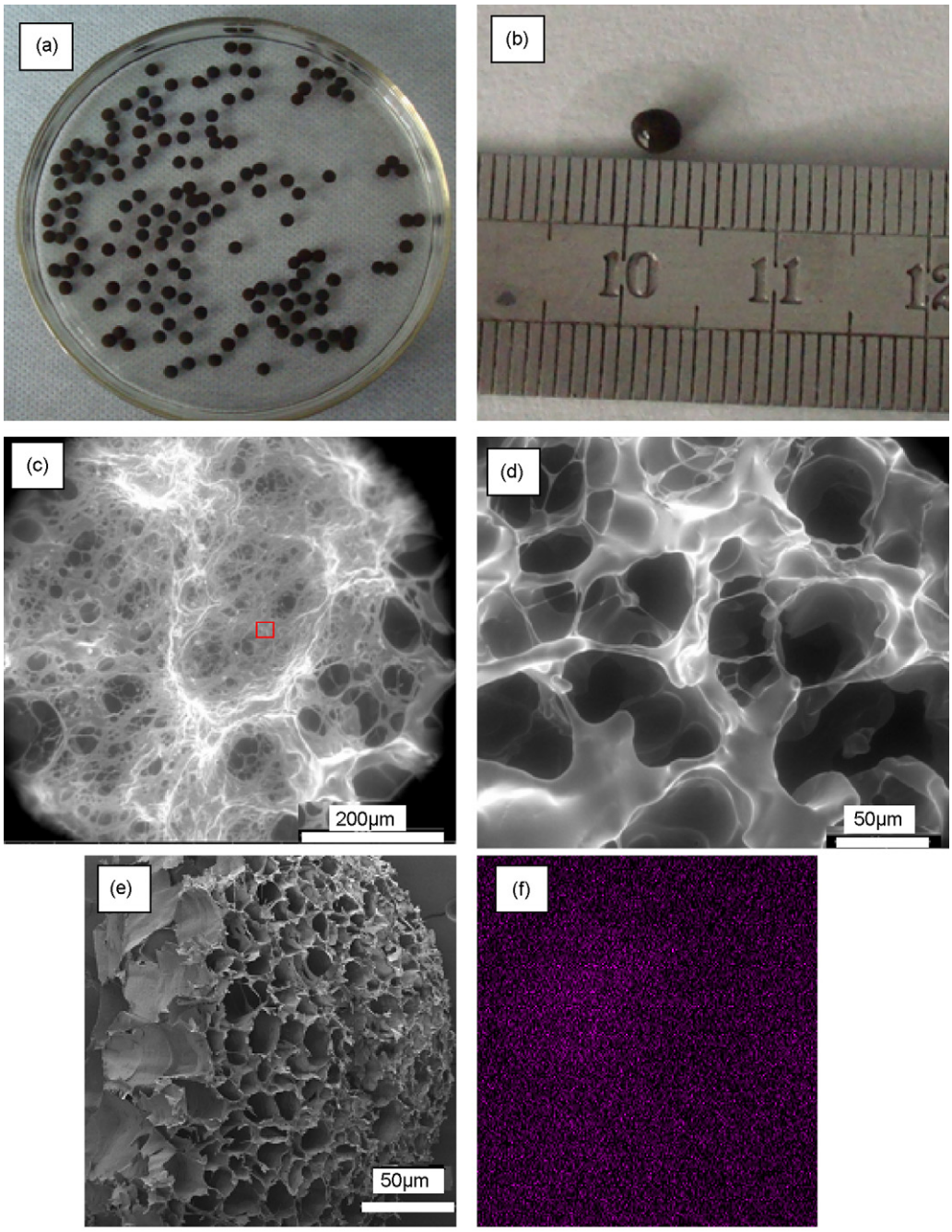

Fig. 1. The size and morphology of CS-NZVI beads was analyzed. (a) The macroscopic shape of CS-NZVI beads; (b) the CS-NZVI beads were uniform and the size of a bead was about 3.1 mm in wet; (c) SEM image of the wet beads. The section was taken through the center of the bead: (d) higher magnification of SEM image of (c) bead; (e) higher magnification of SEM image of (c) bead in dry; (f) X-ray element map of Fe in the region of (c) in the red frame. (For interpretation of the references to color in this figure legend, the reader is referred to the web version of this article.)

ethanol and HCl were provided by First Chemical Reagent Manufactory (Tianjin, China). All other chemicals were of analytical grade purity. Deionised (DI) water was used to prepare all solutions.

2.2. Preparation of CS-NZVI beads

CS-NZVI beads were prepared according to the procedures described in detail elsewhere [19]. Briefly, chitosan flake (1.0 g) was dissolved in 100 mL 1.0% (v/v) acetic acid solution at 60 °C. As the chitosan solution was cooled down to 20 °C, a 0.5 g amount of NZVI was gently added into the solution. Then, the mixture was promptly dropped into a 2 M NaOH solution to form CS-NZVI beads. The beads were retained in the deoxygenated NaOH solution for 24 h for hardening and then washed with deionised water. The whole process was carried out in a nitrogen atmosphere.

2.3. NZVI characterization and analytical methods

The size distribution of CS-NZVI beads was measured visually with a ruler. The morphological analysis of the beads was performed using a scanning electron microscope (SEM) with energy-dispersive X-ray (EDS) detection (SEM/EDS, Philips XL-30 TMP). A little part in the center of the bead was used for the analysis of X-ray element map of Fe. Fourier transform infrared (FTIR)

spectra for the CS-NZVI beads before and after their exposure to Cr (VI) were obtained using a Nexus FTIR spectroscopy. The CS-NZVI samples were also used to the X-ray photoelectron spectroscope analysis (XPS).

Total chromium was measured using inductively coupled air-acetylene flame atomic emission spectrometry (AAF-AES) (WFX-130, BJR Co.). The concentration of Cr (VI) in the solution was determined using a UV/visible spectrophotometer and by the diphenylcarbazine method [15].

2.4. Cr (VI) removal experiments

Batch experiments for removal of Cr (VI) in water were carried out in polytetrafluoro ethylene bottles at atmospheric pressure. To each bottle, 100 mL Cr (VI) (20 mg/L) solution and CS-NZVI beads (entrapped NZVI by 100 mL mixture of chitosan and acetic acid) were added. Sampling was made at certain time-interval and the samples were filtered through a 0.22 μm filter. All experiments were performed in duplicate.

3. Results and discussion

3.1. SEM characterization

Fig. 1(a) and (b) shows that CS-NZVI beads are nearly spherical in shape and uniform in size with a mean diameter of 3.1 mm. CS-NZVI beads are black because of entrapment of NZVI particles in CS beads. Fig. 1(c) reveals that CS-NZVI beads are macroporous and the pore sizes in the CS-NZVI beads are heterogeneous because reaction between NaOH and acetic acid is not uniform throughout the beads. Analysis of SEM images (Fig. 1(c) and (d)) indicates that the pore size ranges from 9.5 to 108.8 μm with an average aperture size of around 28.6 μm. Guo et al. reported the pore size on the surfaces of CS beads to be 4.9–15.8 μm [21]. The pore size of the CS-NZVI beads in this work is bigger than that of the CS beads. The bigger pore size in the CS-NZVI beads facilitates the mass transfer between these beads and wastewater. The higher magnification of SEM image of CS-NZVI beads in dry form (Fig. 1(e)) shows that the pore size of the dry beads becomes smaller than that of the wet beads.

X-ray element map of Fe (Fig. 1(f)) shows that NZVI particles are uniformly distributed in the CS-NZVI beads. It suggests that entrapment of NZVI in CS beads can prevent the particles from aggregation. However, Bezbaruah et al. reported high agglomeration of NZVI in parts of the alginate beads [16]. Further, NZVI particles in the CS beads are not oxidised by oxygen or ignite spontaneously when directly exposed to air. It is believed that in CS-NZVI beads system, NZVI particles are better protected by chitosan and oxidation is hindered. Incorporating of amino groups on the chitosan to iron nanoparticles can enhance the stability of the nanoparticles [13].

3.2. Removal mechanism of Cr (VI) by CS-NZVI beads

The removal mechanism of Cr (VI) by CS-NZVI beads can be outlined as in Scheme 1. Because of the free amino groups and hydroxyl groups exposed in chitosan, Cr (VI) can be easily accumulated on the surface or inside of the CS-NZVI beads when the CS-NZVI beads were exposed to the solution of CrO_4^{2-}. Most of CrO_4^{2-} ions entered the CS-NZVI beads a few minutes later, and then reacted with NZVI. The enrichment of Cr (VI) facilitates the reaction between NZVI and Cr (VI). This ion was quickly reduced to Cr (III) and Fe (III) was formed on the surface of NZVI particles.

To identify possible interactions between CS-NZVI beads and Cr (VI), FTIR spectra were obtained for the CS-NZVI beads before and after the beads were exposed to Cr (VI) and the results were shown in Fig. 2. The characteristic peaks at 1631 and 3426 cm^{-1}

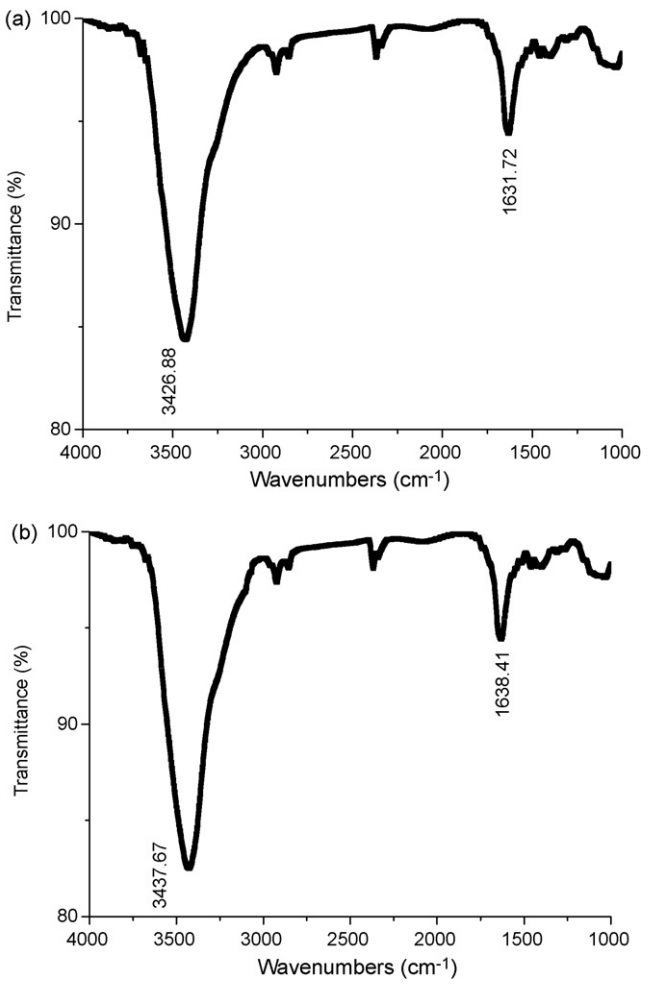

Fig. 2. FTIR spectra for the CS-NZVI beads before and after Cr (VI) reduction: (a) before Cr (VI) reduction and (b) after Cr (VI) reduction. Initial Cr (VI) concentration: 20 mg/L; the concentration of NZVI in CS-NZVI: 5.0 g/L; pH: 6.4; temperature: 20 °C.

for chitosan (Fig. 2 (a)) are contributed to the N–H and O–H bending vibration [22], respectively, indicating the existence of amide (II) and hydroxyl groups in chitosan. After Cr (VI) reduction, the FTIR spectrum for CS-NZVI beads in Fig. 2(b) showed a shift of the peak at 1631–1638 and 3426–3437 cm^{-1}. The results indicate that the functional groups of amide (II) and hydroxyl groups may participate in the Cr (VI) removal process. Cr (VI) can be removed by three forms of chitosan (flakes, beads, and modified beads obtained by glutaraldehyde cross-linking) [23]. The amide (II) and hydroxyl groups of chitosan are the main binding sites for the heavy metal ions [19,24]. The amide (II) and hydroxyl groups of chitosan have a high sorption capacity for Cr (VI) [25]. Hence, it is reasonably proposed that chitosan can enrich Cr (VI) on the surface or inside of the CS-NZVI beads. The enrichment of Cr (VI) contributes immensely to the contact and interaction between Cr (VI) and NZVI due to the macroporous structure of the beads. Therefore, the FTIR spectra in Fig. 2 clearly support the removal mechanism given in Scheme 1.

XPS was employed to test the elemental composition of final products and the results are presented in Figs. 3–5. Fig. 3 shows the typical wide scan XPS spectra for the CS-NZVI beads before and after Cr (VI) reduction. It is clear that a new peak at the banding energy (BE) about 580 eV appeared after Cr (VI) reduction. The presence of the band was designated to the photoelectron peak of chromium and indicated the uptake of chromium on the surface of CS-NZVI beads.

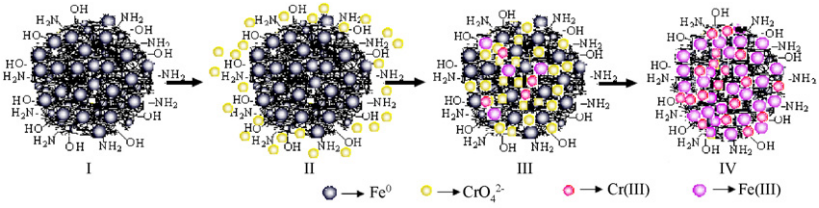

I The fresh CS-NZVI beads were prepared. The free amino groups and hydroxyl groups in chitosan are exposed on the surface of CS-NZVI beads.

II Cr (VI) was easily accumulated on the surface or inside of the CS-NZVI beads when the CS-NZVI beads were exposed to the solution of CrO_4^{2-}.

III Most of CrO_4^{2-} ions entered the CS-NZVI beads a few minutes later, and then reacted with NZVI.

IV The reaction "Fe + Cr(VI) → Fe(III) + Cr(III)" happened quickly and Cr (VI) is reduced to Cr (III) and Fe (III) is the predominant species on the surface of the NZVI particles.

Scheme 1. Schematic diagram showing the removal mechanism of Cr (VI) by CS-NZVI. (I) The fresh CS-NZVI beads were prepared. The free amino groups and hydroxyl groups in chitosan are exposed on the surface of CS-NZVI beads. (II) Cr (VI) was easily accumulated on the surface or inside of the CS-NZVI beads when the CS-NZVI beads were exposed to the solution of CrO_4^{2-}. (III) Most of CrO_4^{2-} ions entered the CS-NZVI beads a few minutes later, and then reacted with NZVI. (IV) The reaction "Fe + Cr(VI) → Fe(III) + Cr(III)" happened quickly and Cr (VI) is reduced to Cr (III) and Fe (III) is the predominant species on the surface of the NZVI particles.

Detailed XPS surveys on the region of Fe2p and Cr2p are presented in Fig. 4. Photoelectron peaks at 710.8 and 724.5 eV (Fig. 4(a)) correspond to the binding energies of $2p_{3/2}$ and $2p_{1/2}$ of oxidised iron [Fe (III)]. The peak at 706.5 eV which can be assigned to Fe^0 [26] is not observed in this work. It signifies that extensive oxidation of iron happens on the surface of NZVI and little Fe^0 is left. Manning et al. and Melitas et al. reported that the oxide of iron on iron surface was γ-FeOOH or α-FeOOH [27,28]. The photoelectron peaks for $Cr2p_{3/2}$ and $Cr2p_{1/2}$ center at 576.8 and 586.4 eV (Fig. 4(b)) and have binding energies and line structures similar to those of Cr (III) [29]. The XPS results suggest that the reduction of Cr (VI) to Cr (III) is complete in less than 1 h.

Fig. 5 shows the detailed XPS N1s spectra for CS-NZVI beads before and after Cr (VI) reduction. It is observed that, before Cr (VI) reduction, there is only one peak at a BE of 398.8 eV (Fig. 5(a)), which could be assigned to the nitrogen atoms in $-NH_2$, but a new peak at BE of 397.0 eV appeared after Cr (VI) reduction (Fig. 5(b)). The new peak at a BE of 397.0 eV can be attributed to the formation of metal–NH_2 complexes (both Fe (III) and Cr (III)), but the intensity of this peak is observed to be very small, indicating that the amount of metal–NH_2 complex, if any, is very limited. Other researchers reported that the presence of the $-NH_2$ and –OH groups on the chitosan surface are behaved either as a mono- or bidentate ligands to coordinate with Fe (III) and Cr (III) [30–31]. The coordinating capability can hinder the formation of Fe(III)–Cr(III) precipitate [13]. However, it is found that the metal–NH_2 complex may be contributed little to hinder the formation of Fe(III)–Cr(III) precipitate in this study. Therefore, the results of Figs. 3–5 clearly support the removal mechanism of Cr (VI) by CS-NZVI beads given in Scheme 1.

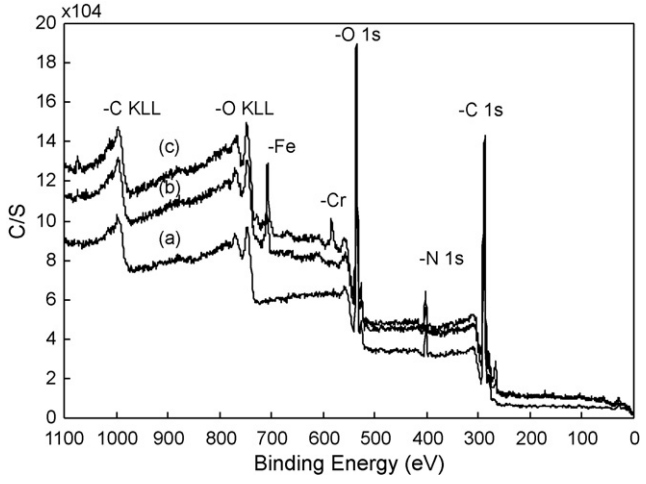

Fig. 3. Typical wide scan XPS spectra for the CS-NZVI beads before and after Cr (VI) reduction: (a) before Cr (VI) reduction and (b) after Cr (VI) reduction. Initial Cr (VI) concentration: 20 mg/L; the concentration of NZVI in CS-NZVI: 5.0 g/L; pH: 6.4; temperature: 20 °C.

3.3. Effect of physicochemical factors on Cr (VI) removal by CS-NZVI beads

3.3.1. Comparison between bare NZVI and entrapped NZVI in Cr (VI) removal

Experiments were conducted to compare the effectiveness of bare NZVI and entrapped NZVI in Cr (VI) removal and the initial concentrations of NZVI and Cr (VI) were 5.0 g/L and 20 mg/L, respectively.

As can be seen, Cr (VI) reduction by entrapped NZVI was observed to be slightly lower compared to bare NZVI in some cases (Fig. 6). For entrapped NZVI and bare NZVI, a marked drop in Cr (VI) concentration in the first 10 min was observed. As in the control (CS beads only), a little drop in Cr (VI) concentration in the first 10 min may also help us to explain the reduction mechanism previously. According to the reduction mechanism, the co-operation of chitosan and NZVI in the CS-NZVI-beads system is favorable for the removal of Cr (VI), and hence the removal rates of Cr (VI) by CS-NZVI beads do not decrease comparing to bare NZVI. Bezbaruah et al. reported that the reactivity of entrapped NZVI in calcium alginate beads was comparable to bare NZVI [16].

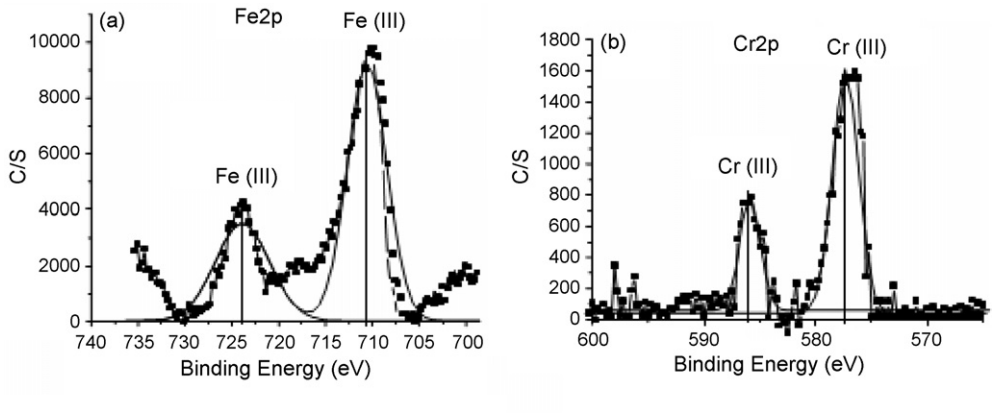

Fig. 4. High-resolution XPS survey of (a) Fe2p and (b) Cr2p of CS-NZVI beads after reacting with 50 mg/L Cr (VI) for 1 h. Initial Cr (VI) concentration: 20 mg/L; the concentration of NZVI in CS-NZVI: 5.0 g/L; pH: 6.4; temperature: 20 °C.

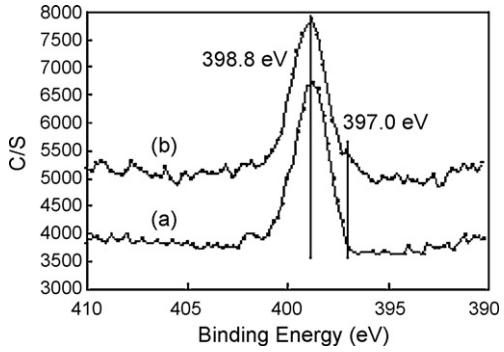

Fig. 5. High-resolution XPS survey of N1s for the CS-NZVI beads before and after Cr (VI) reduction: (a) before Cr (VI) reduction and (b) after Cr (VI) reduction. Initial Cr (VI) concentration: 20 mg/L; the concentration of NZVI in CS-NZVI: 5.0 g/L; pH: 6.4; temperature: 20 °C.

3.3.2. *Effect of NZVI dosages entrapped in the CS beads on Cr (VI) removal*

The influence of NZVI dosages on the removal rates of Cr (VI) was investigated, and the results are shown in Figs. 7 and 8. For 100 mL of 20 mg/L initial Cr (VI) concentration and 3.0–12.0 g/L NZVI, the values of the rate constants are 0.022, 0.062, 0.0772, and 0.0908 min^{-1}, respectively. Obviously, κ_{obs} displays a good linearity to the dosage of NZVI ($R^2 > 0.98$), and the removal of Cr (VI) by CS-NZVI beads follows pseudo-first-order reaction kinetics (Fig. 7).

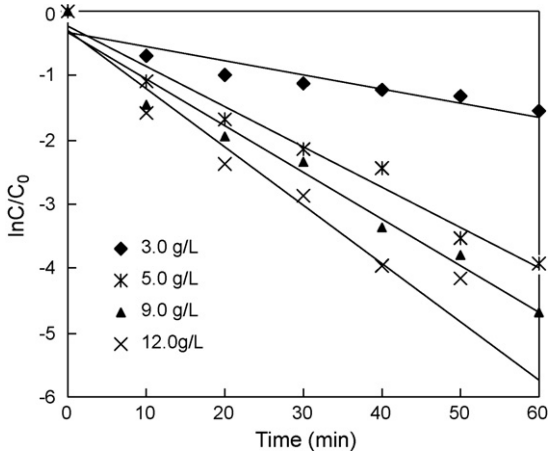

Fig. 7. Kinetics of removal of Cr (VI) by CS-NZVI beads. Initial Cr (VI) concentration: 20 mg/L; the concentration of NZVI in CS-NZVI: 3.0 g/L, 5.0 g/L, 9.0 g/L and 12.0 g/L; pH: 6.4; temperature: 20 °C.

The reductions of Cr (VI) in other Fe^0 system have been reported as pseudo-first-order reaction [28].

However, when a support is introduced into the reduction of Cr (VI), complicated kinetic behavior is noticed in our study and also in the investigations by other researchers [15]. In our study, there

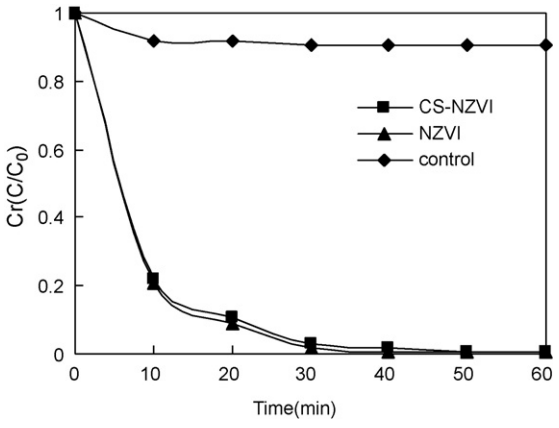

Fig. 6. Removal rates of Cr (VI) by CS-NZVI beads and bare NZVI. Initial Cr (VI) concentration: 20 mg/L; bare NZVI dosages: 5.0 g/L; the concentration of NZVI in CS-NZVI: 5.0 g/L; pH: 6.4; temperature: 20 °C.

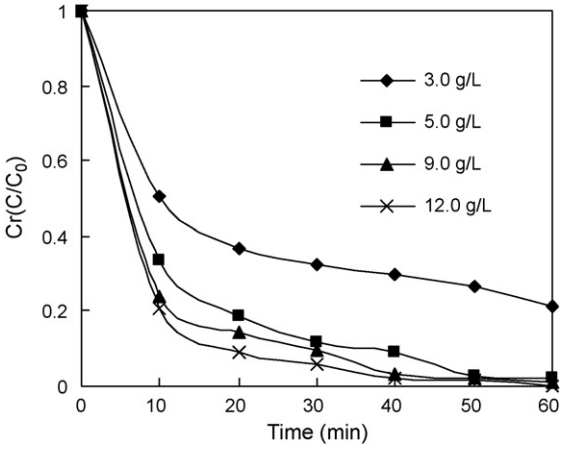

Fig. 8. Effect of nanoparticle dosage on Cr (VI) removal by CS-NZVI beads. Initial Cr (VI) concentration: 20 mg/L; the concentration of NZVI in CS-NZVI: 3.0 g/L, 5.0 g/L, 9.0 g/L and 12.0 g/L; pH: 6.4; temperature: 20 °C.

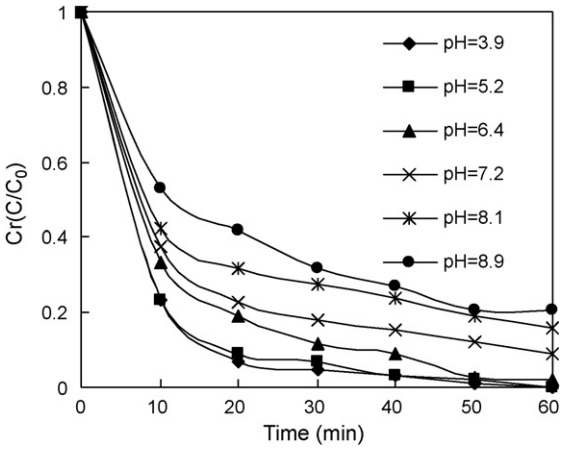

Fig. 9. Effect of pH values on Cr (VI) removal by CS-NZVI beads. Initial Cr (VI) concentration: 20 mg/L; the concentration of NZVI in CS-NZVI: 5.0 g/L; pH: 3.9, 5.2, 6.4, 7.2, 8.1 and 8.9; temperature: 20 °C.

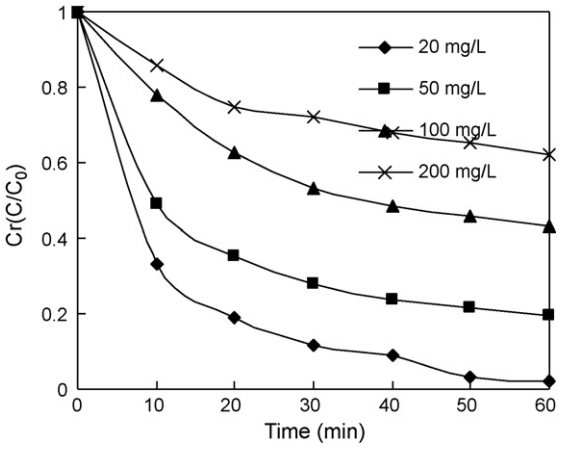

Fig. 10. Effect of initial Cr (VI) concentration on Cr (VI) removal by CS-NZVI beads. Initial Cr (VI) concentration: 20 mg/L, 50 mg/L, 100 mg/L and 200 mg/L; the concentration of NZVI in CS-NZVI: 5.0 g/L; pH: 6.4; temperature: 20 °C.

should be a faster physical adsorption by chitosan and a chemical adsorption by NZVI in the first 10 min of the experiment, which can be seen from Fig. 6 and the reduction mechanism.

Fig. 8 shows that increasing the amount of NZVI results in a faster and more extended removal of the Cr (VI) from the aqueous phase. At an initial concentration of 3.0, 5.0, 9.0, and 12.0 g/L NZVI, about 70.4%, 90.2%, 96.8% and 98.4% of the Cr (VI) are removed within 40 min, respectively. This is mainly due to that an increase in the dosage of NZVI nanoparticles can lead to an increase in total surface area and available active sites for Cr (VI) [27]. Hence, about 20% more Cr (VI) removal is achieved when the dosage of NZVI nanoparticles is increased from 3.0 to 5.0 g/L. However, for a fixed Cr (VI) dosage, the total Cr (VI) available to NZVI nanoparticles is limited when the dosage of NZVI nanoparticles is excess. As a result, the removal rate increases only 1.6% when the dosage of NZVI increases from 9.0 to 12.0 g/L.

3.3.3. Effect of pH values on Cr (VI) removal

The effect of pH on Cr (VI) removal by CS-NZVI beads is shown in Fig. 9. It is observed that with an increase of pH from 3.9 to 8.9, the removal rate decreases gradually. Cr (VI) exists primarily as salts of H_2CrO_4, $HCrO_4^-$ and CrO_4^{2-} depending on the pH. H_2CrO_4 predominates at pH less than 1.0, $HCrO_4^-$ at pH between 1.0 and 6.0, and CrO_4^{2-} pH above about 6.0 [32]. According following reaction (Eq. (1)) [33], the decrease of pH can accelerate the reaction rate of iron oxidation. The lower pH also can prevent the formation of Fe(III)–Cr(III) precipitate. Thus Cr (VI) removal rate increases with an increase of pH values.

$$Fe^0 + CrO_4^{2-} + 4H_2O = Cr(OH)_3 + Fe(OH)_3 + 2OH^- \quad (1)$$

Furthermore, at lower pH the sorbent is positively charged due to the protonation of amino groups, while the sorbate, Cr (VI), exists mostly as an anion leading to the electrostatic attraction between sorbent and sorbate [25]. Therefore, the electrostatic attraction between the positive chargers of NZVI and the negatively charged chromate anion facilitates the adsorption of Cr (VI) and enhances the reduction of Cr (VI) to Cr (III) [34].

3.3.4. Effect of initial Cr (VI) concentration on Cr (VI) removal

The effect of initial Cr (VI) concentration on Cr (VI) removal is shown in Fig. 10. It can be observed that the removal rate of Cr (VI) decreases with an increase of the initial Cr (VI) concentration. It has been reported that since Cr (VI) is a strong oxidant and a well-known passivator of Fe^0, as more Cr (VI) came closely to Fe^0, more Fe^0 would be oxidised and lost their activity leading to the decrease in the removal rate [35]. $Fe_{(1-x)}Cr_{(x)}(OOH)_3$ formed on the surface of NZVI will reduce the electron transfer from NZVI to Cr (VI) and accordingly retard Cr (VI) reduction [29,36]. Furthermore, for a fixed adsorbent dose, the total available adsorption sites are limited thus leading to a decrease in percentage removal of adsorbate corresponding to an increased initial adsorbate concentration [37].

3.3.5. Effect of reaction temperature on Cr (VI) removal

The effect of the temperature on the Cr (VI) removal was investigated at four different temperatures, i.e., from 15 to 30 °C. Fig. 11 shows that Cr (VI) removal rates increase as an increase of the temperature from 15 to 30 °C. Vibration rate of Cr (VI) increases with the increase in temperature thus leading to a higher colliding frequency between Cr (VI) and CS-NZVI beads [38]. At a high temperature, more Cr (VI) diffuses into the beads and is reduced to Cr (III) by NZVI at the accelerated rate. In addition, an increase in the temperature is favorable for the transfer of electrons from NZVI to Cr (VI) [39]. As a result, a fraction of Cr (VI) in the solution will be quickly reduced to Cr (III).

The results clearly indicate that entrapment of NZVI in CS beads prevents the particles from aggregation and oxidation. The reactivity of entrapped NZVI in CS beads was comparable to bare NZVI, and the Cr (VI) can be rapidly removed from wastewater. How-

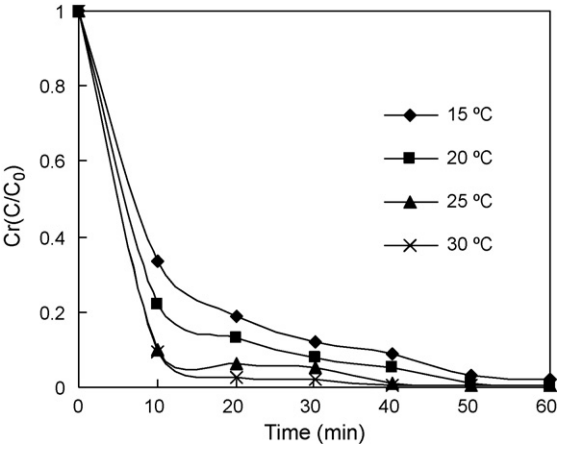

Fig. 11. Effect of reaction temperature on Cr (VI) removal by CS-NZVI beads. Initial Cr (VI) concentration: 20 mg/L; the concentration of NZVI in CS-NZVI: 5.0 g/L; pH: 6.4; temperature: 15 °C, 20 °C, 25 °C and 30 °C.

ever, the CS-NZVI beads are soft and the mechanical strength of the beads needs to be improved. Several methods have been used to modify chitosan through either physical or chemical modifications [40–42]. These modifications were proposed to improve pore size, mechanical strength and biocompatility [24,43]. With further improvement in mechanical strength of the CS-NZVI beads, the chitosan entrapment technique may possibly offer a way to effectively use NZVI in many surface water or groundwater remediation situations.

4. Conclusions

In this study, CS-NZVI beads have been successfully prepared and their efficiency in the removal of Cr (VI) under ambient conditions has been evaluated. The removal rates of Cr (VI) using bare NZVI and CS-NZVI beads were 83% and 82%, respectively, over a 30-min period. The study reveals that the removal rates increase with increasing temperature and NZVI dosage but decrease with the increase in initial concentration of Cr (VI) and pH values. The removal mechanism of Cr (VI) by CS-NZVI beads can be proposed that the enrichment of Cr (VI) on the surface or inside of the CS-NZVI beads facilitates the reaction between NZVI and Cr (VI), and hence Cr (VI) was quickly reduced to Cr (III). The free amino groups and hydroxyl groups can coordinate with Fe (III) and Cr (III), but the amount of metal–NH_2 complex, if any, is very limited. Thus the free amino groups and hydroxyl groups on CS may contribute little to hinder the formation of Fe(III)–Cr(III) precipitate.

Acknowledgments

The authors thank Yunxian Liu for her assistance with the measurement of the concentration of Cr (VI), Hui Wang and Fei He for their support with the SEM and XPS analyses. This work was supported in part by the National Natural Science Foundation of China (Grant No. 20776096).

References

[1] M.L. Allan, L.E. Kukacka, Blast furnace slag-modified grouts for in situ stabilization of chromium-contaminated soil, Waste Manage. 15 (3) (1995) 193–202.
[2] J.S. Fruchter, In situ treatment of chromium-contaminated groundwater, Environ. Sci. Technol. 36 (2002) 464A–472A.
[3] W. Wang, Z.H. Jin, T.L. Li, H. Zhang, S. Gao, Preparation of spherical iron nanoclusters in ethanol–water solution for nitrate removal, Chemosphere 65 (8) (2006) 1396–1404.
[4] W.X. Zhang, C.B. Wang, H.L. Lien, Treatment of chlorinated organic contaminants with nanoscale bimetallic particles, Catal. Today 40 (4) (1998) 387–395.
[5] Q.Y. Liu, Y.L. Bei, F. Zhou, Removal of lead (II) from aqueous solution with amino-functionalized nanoscale zero-valent iron, Cent. Eur. Chem. 7 (1) (2009) 79–82.
[6] J.S. Cao, W.X. Zhang, Stabilization of chromium ore processing residue (COPR) with nanoscale iron particles, J. Hazard. Mater. 132 (2–3) (2006) 213–219.
[7] S. Krajangpan, L. Jarabek, J. Jepperson, B. Chisholm, A. Bezbaruah, Polymer modified iron nanoparticles for environmental remediation, Polym. Prepr. 49 (2008) 921.
[8] S.R. Kanel, D. Nepal, B. Manning, H. Choi, Transport of surface-modified nanoparticle in porous media and application to arsenic (III) remediation, J. Nanopart. Res. 9 (2007) 725–735.
[9] J. Quinn, C. Geiger, C. Clausen, K. Brooks, C. Coon, S. O'Hara, T. Krug, D. Major, W.S. Yoon, A. Gavaskar, T. Holdsworth, Field demonstration of DNAPL dehalogenation using emulsified zero-valent iron, Environ. Sci. Technol. 39 (2005) 1309–1318.
[10] D.W. Elliott, W.X. Zhang, Field assessment of nanoscale bimetallic particles for groundwater treatment, Environ. Sci. Technol. 35 (2001) 4922–4926.
[11] F. He, D. Zhao, Preparation and characterization of a new class of starch-stabilized bimetallic nanoparticles for degradation of chlorinated hydrocarbons in water, Environ. Sci. Technol. 39 (2005) 3314–3320.
[12] A. Tiraferri, K.L. Chen, R. Sethi, M. Elimelech, Reduced aggregation and sedimentation of zero-valent iron nanoparticles in the presence of guar gum, J. Colloid Interface Sci. 324 (2008) 71–79.
[13] B. Geng, Z.H. Jin, T.L. Li, X.H. Qi, Kinetics of hexavalent chromium removal from water by chitosan-Fe^0 nanoparticles, Chemosphere 75 (2009) 825–830.
[14] F. He, D.Y. Zhao, J.C. Liu, C.B. Roberts, Stabilization of Fe–Pd nanoparticles with sodium carboxymethyl cellulose for enhanced transport and dechlorination of trichloroethylene in soil and groundwater, Ind. Eng. Chem. Res. 46 (2007) 29–34.
[15] S.M. Ponder, J.C. Darab, T.E. Mallouk, Remediation of Cr (VI) and Pb (II) aqueous solutions using supported, nanoscale zero-valent iron, Environ. Sci. Technol. 34 (2000) 2564–2569.
[16] A.N. Bezbaruah, S. Krajangpan, B.J. Chisholm, E. Khan, J.J. Bermudez, Entrapment of iron nanoparticles in calcium alginate beads for groundwater remediation applications, J. Hazard. Mater. 166 (2009) 1339–1343.
[17] L. Jin, R.B. Bai, Mechanism of lead adsorption on chitosan/PVA hydrogel beads, Langmuir 18 (2002) 9765–9770.
[18] C.L. Lasko, M.P. Hurst, An investigation into the use of chitosan for the removal of soluble silver from industrial wastewater, Environ. Sci. Technol. 33 (1999) 3622–3626.
[19] N. Li, R.B. Bai, Copper adsorption on chitosan–cellulose hydrogel beads: behaviors and mechanisms, Sep. Purif. Technol. 42 (2005) 237–247.
[20] N. Li, R.B. Bai, C.K. Liu, Enhanced, selective adsorption of mercury ions on chitosan beads grafted with polyacrylamide via surface-initiated atom transfer radical polymerization, Langmuir 21 (2005) 11780–11787.
[21] T.Y. Guo, Y.Q. Xia, G.J. Hao, M.D. Song, B.H. Zhang, Adsorptive separation of hemoglobin by molecularly imprinted chitosan beads, Biomaterials 25 (2004) 5905–5912.
[22] Y. Wan, H. Wu, A. Yu, D. Wen, Biodegradable polylactide/chitosan blend membranes, Biomacromolecules 7 (2006) 1362–1372.
[23] L. Dambies, C. Guimon, S. Yiacoumi, E. Guibal, Characterization of metal ion interactions with chitosan by X-ray photoelectron spectroscopy, Colloids Surf. A 177 (2001) 203–214.
[24] E. Guibal, Interaction of ions with chitosan-based sorbents: a review, Sep. Purif. Technol. 38 (2004) 43–74.
[25] V.M. Boddu, K. Abburi, J.L. Talbott, E.D. Smith, Removal of hexavalent chromium from wastewater using a new composite chitosan biosorbent, Environ. Sci. Technol. 37 (2003) 4449–4456.
[26] J.N. Fiedor, W.D. Bostick, R.J. Jarabek, J. Farrell, Understanding the mechanism of uranium removal from groundwater by zero-valent iron using X-ray photoelectron spectroscopy, Environ. Sci. Technol. 32 (1998) 1466–1473.
[27] B.A. Manning, J.R. Kiser, H. Kwon, S.R. Kanel, Spectroscopic investigation of Cr (III) and Cr (VI)-treated nanoscale zero-valent iron, Environ. Sci. Technol. 41 (2007) 586–592.
[28] N. Melitas, O. Chuffe-Moscoso, J. Farrell, Kinetics of soluble chromium removal from contaminated water by zero-valent iron media: corrosion inhibition and passive oxide effects, Environ. Sci. Technol. 35 (2001) 3948–3953.
[29] X.Q. Li, J.S. Cao, W.X. Zhang, Stoichiometry of Cr (VI) immobilization using nanoscale zero-valent iron (nZVI): a study with high-resolution X-ray photoelectron spectroscopy (HR-XPS), Ind. Eng. Chem. Res. 47 (2008) 2131–2139.
[30] A.J. Varma, S.V. Deshpande, J.F. Kennedy, Metal complexation by chitosan and its derivatives: a review, Carbonhydr. Polym. 55 (2004) 77–93.
[31] S.C. Bhatia, N. Ravi, A Mossbauer study of the interaction of thitosan and D-glucosamine with iron and its relevance to other metalloenzymes, Biomacromolecules 4 (2003) 723–727.
[32] D. Mohan, C.U. Pittman Jr., Activated carbons and low cost adsorbents for remediation of tri- and hexavalent chromium from water, J. Hazard. Mater. B 137 (2006) 762–811.
[33] M.J. Alowitz, M.M. Scherer, Kinetics of nitrate, nitrite, and Cr (VI) reduction by iron metal, Environ. Sci. Technol. 36 (2002) 299–306.
[34] T.Y. Liu, L. Zhao, X. Tan, S.J. Liu, J.J. Li, Y. Qi, G.Z. Mao, Effects of physicochemical factors on Cr (VI) removal from leachate by zero-valent iron and a-Fe_2O_3 nanoparticles, Water Sci. Technol. 61 (2010) 2759–2767.
[35] H.H. Uhlig, R.W. Revie, Corrosion and Corrosion Control, John Wiley, New York, 1985.
[36] A.P. Davis, V. Bhatnagar, Adsorption of cadmium and humic acid onto hematite, Chemosphere 30 (1995) 243–256.
[37] T. Hiemstra, W.H. Van-Riemsdijk, Surface structural ion adsorption modeling of competitive binding of oxyanions by metal (hydr)oxides, J. Colloid Interface Sci. 210 (1999) 182–193.
[38] F.W. Chuang, R.A. Larson, M.S. Wessman, Zero-valent iron-promoted dechlorination of polychlorinated biphenyls, Environ. Sci. Technol. 29 (1995) 2460–2463.
[39] A.W. Breed, C.J.N. Dempers, G.E. Searby, M.N. Gardner, D.E. Rawlings, G.S. Hansford, The effect of temperature on the continuous ferrous-iron oxidation kinetics of a predominantly Leptospirillum ferrooxidans culture, Biotechnol. Bioeng. 65 (1999) 44–53.
[40] T. Candy, C.P. Sharma, Chitosan matrix for oral sustained delivery of ampicillin, Biomaterials 14 (1993) 939–944.
[41] R. Mara, B.J. Suder, J.P. Wightman, Interaction of heavy metals with chitin and chitosan: chrominum (III), J. Appl. Polym. Sci. 27 (1982) 4827–4837.
[42] X.Z. Shu, K.J. Zhu, Chitosan/gelatin microsphere prepared by modified emulsification and ionotropic gelation, J. Microencapsulation 18 (2001) 237–245.
[43] X. Zeng, E. Ruckenstein, Cross-linked macroporous chitosan anion-exchange membraned for protein separations, J. Membr. Sci. 148 (1998) 195–205.